Available online at www.sciencedirect.com
SCIENCE DIRECT
International Journal of Heat and Mass Transfer 49 (2006) 1731–1737
International Journal of HEAT and MASS TRANSFER
www.elsevier.com/locate/ijhmt

Condensation from gas–vapour mixtures in small non-circular tubes

S. Krishnaswamy [1], H.S. Wang *, J.W. Rose *

Department of Engineering, Queen Mary, University of London, Mile End Road, London E1 4NS, UK

Received 19 September 2005
Available online 17 January 2006

Abstract

Careful measurements have been made during condensation of steam from steam–air mixtures flowing in a small, flattened, horizontal tube. The ranges of the relevant variables covered (inlet temperature, pressure, air mole fraction and mixture mass flow rate) were chosen to simulate those occurring in an exhaust heat-exchanger tube of a proposed fuel-cell engine. The experimental tube was cooled by water in laminar counter flow to simulate the external heat-transfer coefficient (air flowing over fins) in the application. The total heat-transfer rate was found from the mass flow rate and temperature rise of the coolant. The tube wall temperature was measured by thermocouples attached in grooves along its length. Special arrangements were made to ensure good mixing of the coolant (in laminar flow) prior to measuring the inlet and outlet temperatures. The condensate was separated using a cyclone at exit from the tube. A simple model was developed to predict local and total heat-transfer and condensation rates and local bulk vapour composition, temperature and pressure along the tube in terms of the inlet parameters and the wall temperature distribution. The measured heat-transfer and condensation rates for the tube were found to be in good agreement with the calculated values without having recourse to empirical adjustment.

Keywords: Condensation; Air–steam mixture; Theory; Flattened tube; Heat-transfer

1. Introduction

On-board water management is important for fuel cell-powered motor vehicles. The objective of the present investigation was to develop and validate a model for use in design of an exhaust condenser for an automotive fuel-cell engine. For given inlet conditions (temperature, pressure, composition and flow rate) and specified distribution of wall temperature, the model determines the local heat flux, condensation mass flux, temperature, composition and pressure along the tube. The total condensation and heat-transfer rates for a tube of given length are readily calculated. In the application the model would be used with a standard approach for the external air-side (cross flow with fins) and an iterative scheme used to determine the distribution of wall temperature along the tube.

An apparatus has been designed and built in which steam–air (air for convenience) mixtures were passed through a tube cooled externally by water flowing in an annulus in counter flow. Laminar flow of the coolant was required to simulate the exterior heat-transfer resistance in the application. Special coolant mixing arrangements were made to ensure accurate mean temperatures were obtained at inlet and exit of the coolant stream. Surface temperatures at several positions along the tube were measured by embedded thermocouples. The ranges of temperature, pressure, composition and flow rate covered those anticipated in the application.

The measured condensation and heat-transfer rates for the tube agreed with the calculated values to within 20%. No empirical adjustment to the model was needed.

* Corresponding authors.
E-mail addresses: h.s.wang@qmul.ac.uk (H.S. Wang), j.w.rose@qmul.ac.uk (J.W. Rose).
[1] Present address: Birla Institute of Technology and Science (BITS) Pilani, Goa campus, Zuari Nagar, Goa 403726, India.

0017-9310/$ - see front matter © 2005 Elsevier Ltd. All rights reserved.
doi:10.1016/j.ijheatmasstransfer.2005.10.018

Nomenclature

A	constant in wall temperature distribution, see Eq. (1)
B	constant in wall temperature distribution, see Eq. (1)
C	constant in wall temperature distribution, see Eq. (1)
c_p	specific isobaric heat capacity of vapour–gas mixture
d_h	hydraulic diameter of condensing tube
D	vapour–gas mixture diffusion coefficient
f	friction factor, $f = \tau_i/\left(\frac{1}{2}\rho u^2\right)$
h_{fg}	specific enthalpy of evaporation
j	segment number
k	thermal conductivity of vapour–gas mixture
k_l	thermal conductivity of condensate
m	mass flow rate of vapour–gas mixture
$\dot{m}_c$	local condensation mass flux
M_a	molar mass of non-condensing gas, i.e. air
M_v	molar mass of vapour
Nu	Nusselt number
P_b	bulk pressure of vapour–gas mixture
$P_s(T)$	saturation pressure
Pr	Prandtl number of vapour–gas mixture
$\dot{q}_w$	heat flux to tube wall
Re	Reynolds number
Sc	Schmidt number of vapour–gas mixture, $\mu/\rho D$
Sh	Sherwood number of vapour–gas mixture, $x(\partial W^*/\partial y)_i$
T	thermodynamic temperature
T_i	interface temperature
T_b	bulk temperature of vapour–gas mixture
T_w	wall temperature
u	bulk vapour–gas mixture velocity
W_v	mass fraction of vapour
W_{vi}	mass fraction of vapour at the liquid–gas interface
W^*	$(W_v - W_{vi})/(W_{vb} - W_{vi})$
W_{vb}	bulk stream mass fraction of vapour
ΔT	temperature difference across condensate film
x	distance along tube
Δx	segment length
y	distance normal to tube wall
α_e	external heat-transfer coefficient
α_g	convective surface heat-transfer coefficient for vapour–gas mixture
δ	condensate film thickness
μ	viscosity of vapour–gas mixture
μ_l	viscosity of condensate
ρ	density of vapour–gas mixture
ρ_l	density of condensate
τ_i	shear stress on condensate film

Subscripts

a	air
b	bulk
c	condensing
i	interface
in	inlet to tube
j	at entry to segment j
l	condensate
s	saturation
v	vapour
w	wall

2. Apparatus and procedure

A flow diagram of the apparatus is shown in Fig. 1. Steam was generated in a stainless steel evaporator fitted with two stainless steel sheathed 1 kW electric heaters. Air was injected via a humidity measuring box and flow meter through a sparge tube at the base of the evaporator. A carry-over suppressor, superheater (500 W) and mixer were located at exit from the evaporator. Temperature and pressure were measured at the tube inlet and exit. The length and hydraulic diameter of the tube were 1 m and 3 mm, respectively. A cyclone separator was located at the tube exit to separate the condensate which was lead to a measuring cylinder while the saturated air was removed via an exit at the top of the separator. The apparatus was well insulated. Cooling water, supplied from a constant head tank, passed through a flow meter, heater and mixer to the PTFE (polytetrafluoroethylene or Teflon) casing holding the tube so that the coolant flowed in the annular space well insulated externally. A mixer was also located at the coolant exit prior to temperature measurement. As well as the inlet and exit coolant temperatures, the inlet-to-exit temperature difference was measured directly using a 10-junction thermopile. All thermocouples were calibrated against a platinum resistance thermometer in a high precision constant temperature bath. Special attention was paid to adequacy of isothermal immersion of all thermocouple junctions. Full details of the apparatus are given by Krishnaswamy [1].

The problem of obtaining accurate mixed mean fluid temperatures in laminar flow has been highlighted by Fujii [2]. For this purpose mixers were used which consisted of a PTFE body with an internal copper tube in which were located, at intervals, brass baffles with holes alternately near the centre and perimeter as shown. Fig. 2 shows detail of a mixer fitted with traversing thermocouples for performance testing. Fig. 3 shows the simple test apparatus in which water was supplied to the mixer from an exter-

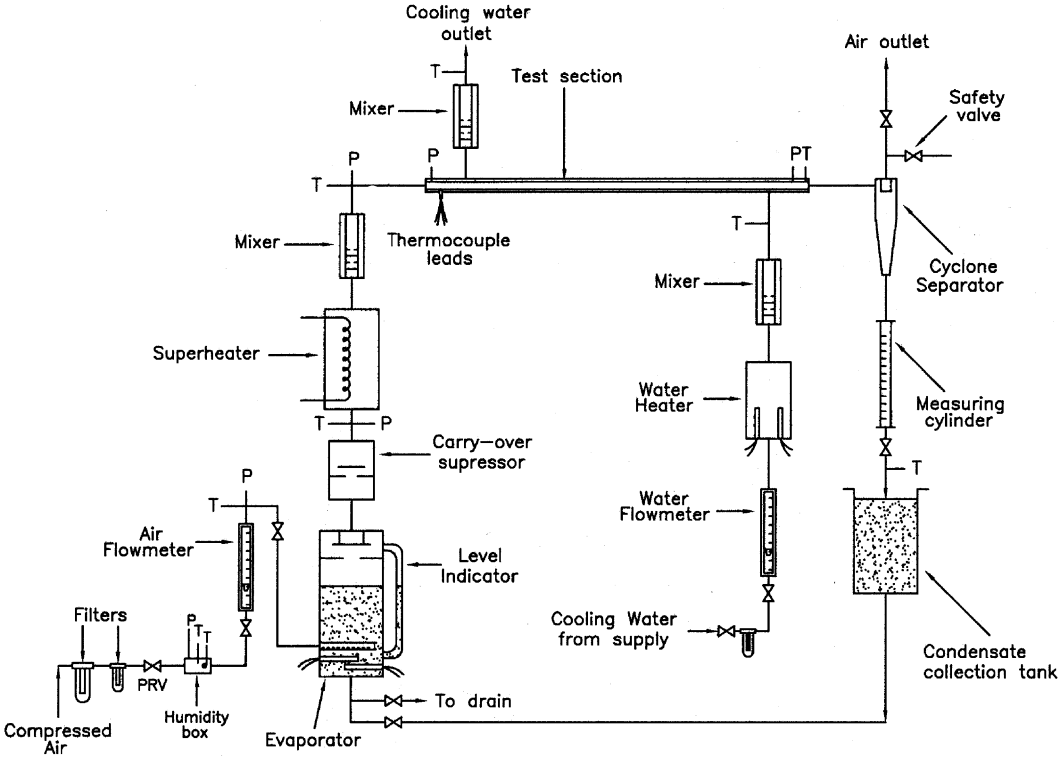

Fig. 1. Flow diagram of test rig.

nally-heated tube. Specimen temperature profiles across inlet and exit of the mixer are shown in Fig. 4 which clearly indicates both the necessity for mixing arrangements and the satisfactory performance of the design adopted.

All measurements were made under steady conditions. The air mass flow rate was measured directly using the flow meter with appropriate temperature and pressure corrections. The steam mass flow rate was found using an energy balance (steady state power required to evaporate steam plus power required to heat the air in steady flow set equal to the evaporator input power) incorporating a small predetermined (as in [3]) heat loss to the surroundings between the evaporator and the test section inlet. To assess the reliability of the apparatus and method, tests were first preformed using only steam. The heat-transfer rate from the tube, as measured by the coolant flow rate and temperature rise, agreed in all cases with that found from an energy balance for the stream flowing through the tube to within 2.5%. The evaporation rate agreed with the condensate collected to within 1%. Ninety four test runs were then made with steam–air mixtures covering the ranges of inlet pressure, temperature, steam mole fraction, steam–air flow rate and coolant inlet temperature which would be used in the application. A measured wall temperature distribution in a typical run is illustrated in Fig. 5. The temperature distributions were fitted by equations of the form:

$$T = A\mathrm{e}^{-Bx} + C \tag{1}$$

where A, B and C are constants, for use when making comparisons with the model.

3. Model

For the high gas concentrations in the exhaust stream and consequent low condensation mass fluxes, the expected condensation regime is a thin laminar film on the tube wall. For the conditions of the test runs the maximum calculated condensate film thickness (at the end of the tube for the highest condensation rate case) was 0.07 mm. The flow rate range and channel dimensions indicated that the gas–vapour flow should be turbulent. For the conditions of the test runs the lowest air–steam Reynolds number was around 3400. With these considerations a simple model, applicable to any gas–vapour mixture, has been developed using well-established, heat-mass transfer analogy methods.

The problem is illustrated in Fig. 6. The tube is divided into segments of given step length. While the wall temperature is higher than the local saturation temperature of the vapour at its partial pressure, the single-phase, gas–vapour flow is treated using the correlation of Gnielinski [4]:

$$Nu = \frac{\alpha_g d_h}{k} = \frac{(f/2)(Re - 1000)Pr}{1 + 12.7(f/2)^{0.5}(Pr^{2/3} - 1)} \tag{2}$$

The friction factor in Eq. (2) and, hence pressure drop, were obtained from the Filonenko [5] correlation:

$$f = (1.58 \ln Re - 3.28)^{-2} \tag{3}$$

and

$$\tau_i = \frac{1}{2} f \rho u^2 \tag{4}$$

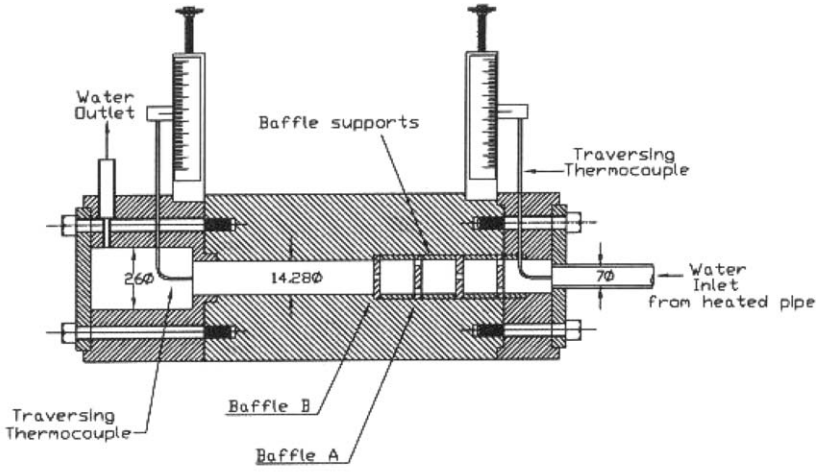

Baffle A	Baffle B
R = 9.14 mm	R = 9.14 mm
PCD = 12 mm	PCD = 6 mm
8 holes, 2 mm dia.	5 holes, 2.5 mm dia.

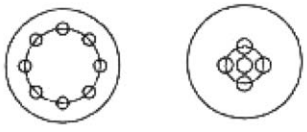

Distance between baffles: 14 mm
Baffle thickness: 3 mm

All dimensions are in mm

Material of construction

1. Baffle: Brass
2. Baffle supports: Copper
3. Water (inlet/outlet) pipe: Copper
4. Mixer body and end pieces: PTFE

Fig. 2. Coolant mixing box fitted with traversing thermocouples for performance testing.

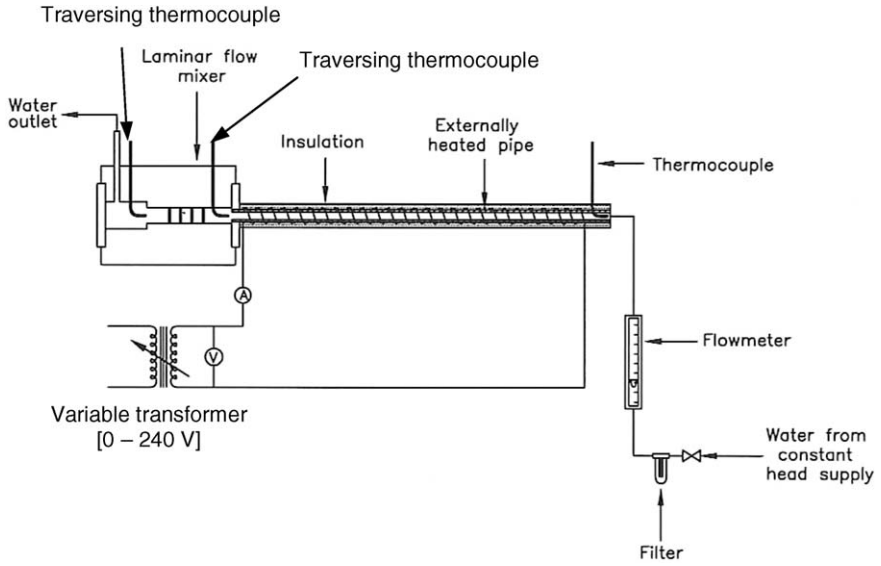

Fig. 3. Test rig for laminar flow mixing box.

Momentum and energy balances for a segment give the temperature and pressure at the entry to the succeeding segment (and hence the temperature and pressure distribution along the channel) as well as the heat-transfer rate to the wall. When the wall temperature just becomes lower than the equilibrium saturation temperature (dew point)

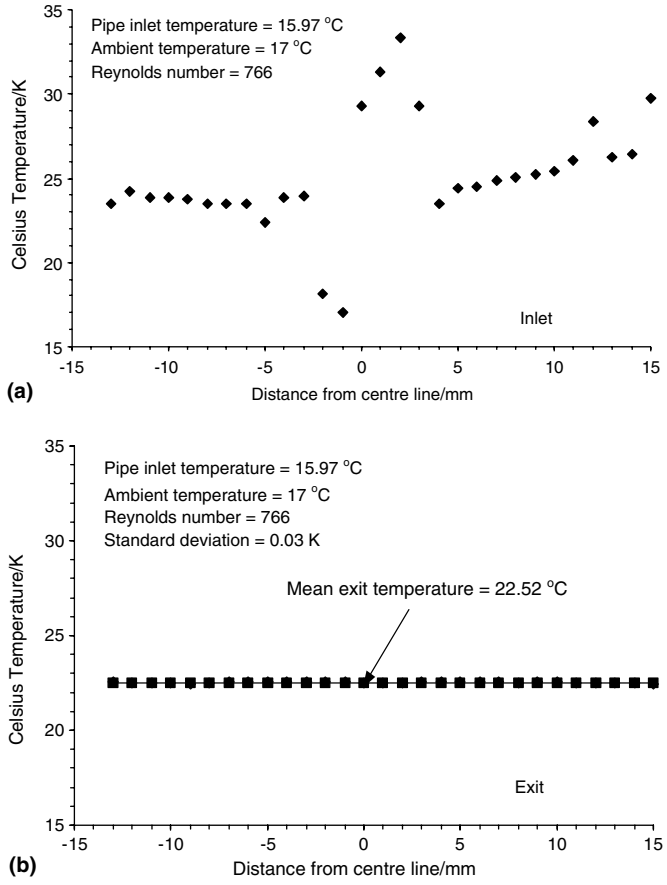

Fig. 4. Specimen temperature profiles across the inlet and outlet of mixer (a) across inlet to mixer (b) across outlet from mixer.

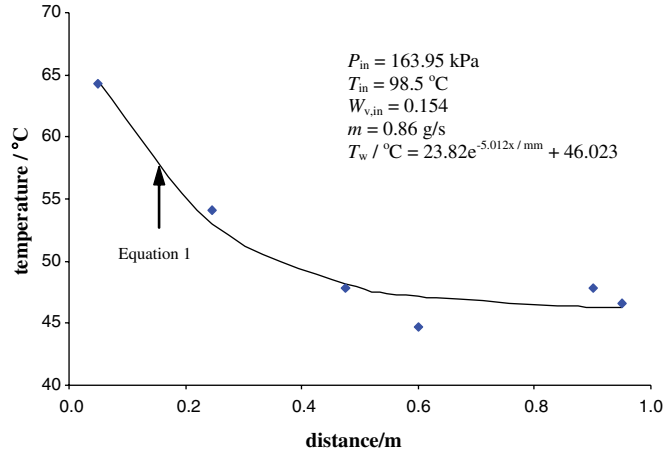

Fig. 5. Specimen measured wall temperature distribution along the condensing tube with curve fit.

condensation commences. Neglecting gravity, the Nusselt approximations give, for the condensate film

$$\frac{\mathrm{d}}{\mathrm{d}x}(\tau_{\mathrm{i}}\delta^2) = \frac{2\mu_{\mathrm{l}}k_{\mathrm{l}}\Delta T}{\rho_{\mathrm{l}}h_{\mathrm{fg}}\delta} \tag{5}$$

from which the finite difference equation may be rearranged to give

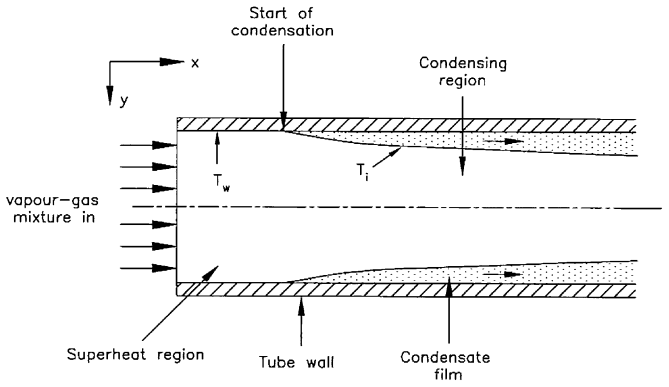

Fig. 6. Schematic view of physical model.

$$\delta_{j+1} = \sqrt{\frac{\left(\frac{2\mu_{\mathrm{l},j}k_{\mathrm{l},j}\Delta T_j\Delta x}{\rho_{\mathrm{l},j}\delta_{j+1}h_{\mathrm{fg},j}}\right) + \tau_{\mathrm{i},j}\delta_j^2}{\tau_{\mathrm{i},j+1}}} \tag{6}$$

The friction factor and surface shear stress were again obtained from Eqs. (3) and (4). Correction to take account of "suction" as described by Kays and Crawford [6] was incorporated, but had negligible effect for the small condensation rates for the conditions investigated. The convective heat transfer from the bulk gas–vapour stream to the condensate surface was found using Eq. (2). Again, correction for "suction" was included but had negligible effect (for details see [1]). For the element under consideration the heat transfer by convection from the gas and resulting from condensation was equated to the wall heat flux thus:

$$\dot{q}_{\mathrm{w}} = \frac{k_{\mathrm{l}}\Delta T}{\delta} = \dot{m}_{\mathrm{c}}h_{\mathrm{fg}} + \alpha_{\mathrm{g}}(T_{\mathrm{b}} - T_{\mathrm{i}}) \tag{7}$$

The condensation mass flux was obtained from

$$Sh = \left(\frac{\dot{m}_{\mathrm{c}}d_{\mathrm{h}}}{\rho D}\right)\frac{1 - W_{\mathrm{vi}}}{(W_{\mathrm{vb}} - W_{\mathrm{vi}})} \tag{8}$$

which arises from the diffusion equation with the impermeability condition for the non-condensing gas at the interface. Sh was obtained by analogy (valid for low condensation rates) from Eq. (2) writing Sh for Nu and Sc for Pr and the mass fraction of gas at the condensate surface is given by the interface equilibrium condition for ideal gas mixtures:

$$W_{\mathrm{ai}} = \frac{P_{\mathrm{b}} - P_{\mathrm{s}}(T_{\mathrm{i}})}{P_{\mathrm{b}} - \left[1 - \left(\frac{M_{\mathrm{v}}}{M_{\mathrm{a}}}\right)\right]P_{\mathrm{s}}(T_{\mathrm{i}})} \tag{9}$$

Eqs. (6)–(9) were solved by a suitable iterative scheme to give the local condensate film thickness, the interface temperature and composition and the condensation mass flux. Momentum, energy and mass balances for the bulk gas–vapour stream gave the pressure, temperature and composition at exit from an element to be used as the entry values for the succeeding element. Properties of the vapour–gas mixtures were taken as the average of their values at the interface and in the bulk. However the difference in the predictions when bulk properties were used were negli-

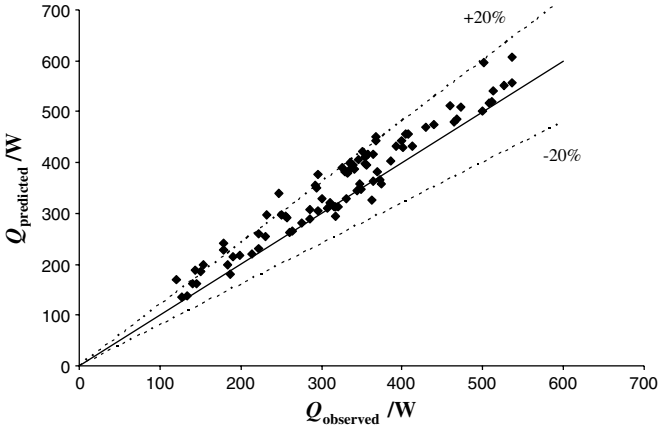

Fig. 7. Comparison of predicted and experimental heat transfer rates.

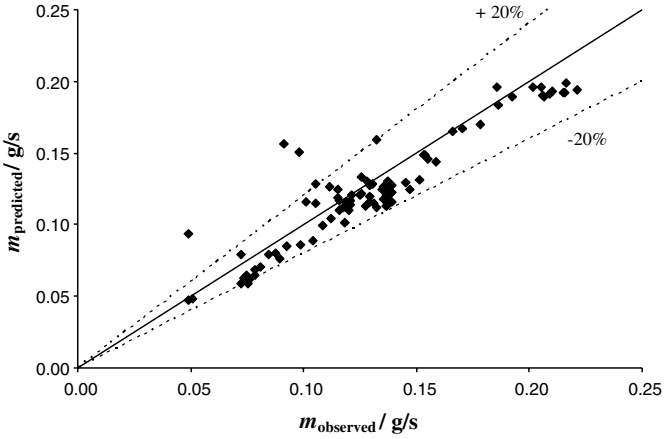

Fig. 8. Comparison of predicted and experimental condensation rates.

gible in comparison with the scatter in Figs. 7 and 8. Condensate properties were taken at reference temperature $(2/3)T_w + (1/3)T_i$. The specific latent heat was taken at T_i.

The whole process was repeated using smaller step lengths until satisfactory convergence was obtained. Properties were taken, for convenience, at the inlet to each segment.

4. Comparison with experiments and specimen results for a tube in a condenser unit

The experimental data are compared with the model calculations in Figs. 7 and 8. It is seen that the model predicts both heat transfer and condensation rate generally within about 20% tending generally to over predict the heat transfer. However, these results were considered satisfactory for design purposes and no empirical adjustment of the model was considered necessary.

In designing a condenser, the tube wall distribution is unknown. For given external air flow rate and fin geometry, an effective lumped external heat-transfer coefficient can be estimated by hand-book methods. When the tube wall resistance is also included in the external heat-transfer coefficient α_a, the local heat flux at any position along the tube may be written

$$q = \alpha_a(T_w - T_a) \tag{10}$$

where T_w is the inside wall temperature and T_a is the external air temperature. An iterative scheme may then be used to determine T_w by equating, at each step, the heat flux using the model as described above for the internal heat and mass transfer problem to that given by Eq. (10). This has been done as an illustration using typical conditions:

External air temperature	43.3 °C
External effective heat-transfer coefficient	130 W/m^2 K
Internal hydraulic diameter of tube	2.98 mm
Length of tube	0.863 m
Condenser tube inlet conditions	
Mass flow rate ($N_2 + H_2O$)	0.83 g/s
Absolute pressure	137.9 kPa
Temperature	204.4 °C
Steam mole fraction (mass fraction)	0.35 (0.26)

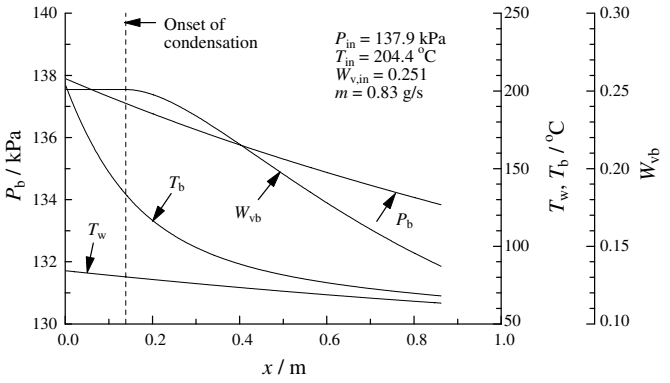

Fig. 9. Specimen distributions of bulk pressure, temperature and vapour mass fraction inside a tube of a condenser unit.

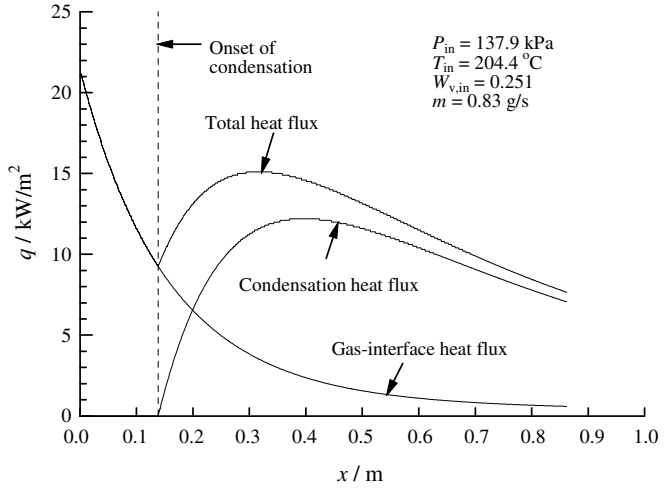

Fig. 10. Specimen distributions of heat fluxes inside a tube of a condenser unit.

The results are shown in Fig. 9, which gives the calculated distributions of T_w, T_b, P_b, and W_{vb} along the tube and Fig. 10 which shows the calculated heat flux distributions along the tube. The calculated total heat-transfer and condensation rates were 396 W and 0.11 g/s.

5. Conclusion

A simple model for predicting the heat transfer and condensation rate for flow of a gas–vapour mixture along a small tube has been developed. For the range of variables studied (those anticipated in a vehicle fuel cell exhaust) the model is in satisfactory agreement with experiment.

Acknowledgements

The authors gratefully acknowledge financial support from the Modine Manufacturing Company, Racine, WI, USA and the UK Engineering and Physical Sciences Research Council.

References

[1] S. Krishnaswamy, Filmwise condensation inside a non-circular horizontal tube in the presence of forced convection and a non-condensing gas. PhD Thesis, University of London, UK, 2004.
[2] T. Fujii, Overlooked factors and unsolved problems in experimental research on condensation heat transfer, Exp. Thermal Fluid Sci. 5 (1992) 652–663.
[3] W.C. Lee, J.W. Rose, Forced-convection condensation on a horizontal tube with and without non-condensing gas, Int. J. Heat Mass Transfer 27 (1984) 519–528.
[4] V. Gnielinski, New equations for heat and mass transfer in turbulent pipe and channel flow, Int. Chem. Eng. 16 (1976) 359–368.
[5] G.K. Filonenko, Hydraulic Resistance in Pipes, Teploergetica 1 (1954) 40–44 (in Russian).
[6] M.W. Kays, M.E. Crawford, Convective Heat and Mass Transfer, third ed., McGraw-Hill, 1993.